British Journal of Pharmacology (2007) 151, 551–563

0007–1188/07 $30.00
www.brjpharmacol.org

RESEARCH PAPER

Anandamide and NADA bi-directionally modulate presynaptic Ca^{2+} levels and transmitter release in the hippocampus

A Köfalvi[1,2], MF Pereira[1], N Rebola[1], RJ Rodrigues[1,3], CR Oliveira[1] and RA Cunha[1]

[1]*Center for Neurosciences of Coimbra, University of Coimbra, Coimbra, Portugal and* [2]*Instituto de Investigação Interdisciplinar, University of Coimbra, Coimbra, Portugal*

Background and purpose: Inhibitory CB_1 cannabinoid receptors and excitatory $TRPV_1$ vanilloid receptors are abundant in the hippocampus. We tested if two known hybrid endocannabinoid/endovanilloid substances, N-arachidonoyl-dopamine (NADA) and anandamide (AEA), presynapticaly increased or decreased intracellular calcium level ($[Ca^{2+}]_i$) and GABA and glutamate release in the hippocampus.
Experimental approach: Resting and K^+-evoked levels of $[Ca^{2+}]_i$ and the release of [^{3}H]GABA and [^{3}H]glutamate were measured in rat hippocampal nerve terminals.
Key results: NADA and AEA *per se* triggered a rise of $[Ca^{2+}]_i$ and the release of both transmitters in a concentration- and external Ca^{2+}-dependent fashion, but independently of $TRPV_1$, CB_1, CB_2, or dopamine receptors, arachidonate-regulated Ca^{2+}-currents, intracellular Ca^{2+} stores, and fatty acid metabolism. AEA was recently reported to block TASK-3 potassium channels thereby depolarizing membranes. Common inhibitors of TASK-3, Zn^{2+}, Ruthenium Red, and low pH mimicked the excitatory effects of AEA and NADA, suggesting that their effects on $[Ca^{2+}]_i$ and transmitter levels may be attributable to membrane depolarization upon TASK-3 blockade. The K^+-evoked Ca^{2+} entry and Ca^{2+}-dependent transmitter release were inhibited by nanomolar concentrations of the CB_1 receptor agonist WIN55212-2; this action was sensitive to the selective CB_1 receptor antagonist AM251. However, in the low micromolar range, WIN55212-2, NADA and AEA inhibited the K^+-evoked Ca^{2+} entry and transmitter release independently of CB_1 receptors, possibly through direct Ca^{2+} channel blockade.
Conclusions and implications: We report here for hybrid endocannabinoid/endovanilloid ligands novel dual functions which were qualitatively similar to activation of CB_1 or $TRPV_1$ receptors, but were mediated through interactions with different targets.
British Journal of Pharmacology (2007) **151,** 551–563; doi:10.1038/sj.bjp.0707252; published online 16 April 2007

Keywords: *N*-arachidonoyl dopamine; anandamide; calcium; GABA; glutamate; hippocampus; nerve terminals

Abbreviations: 2APB, 2-aminoethoxydiphenyl borate; AEA, arachidonoylethanolamide (anandamide); CB_1, cannabinoid type-1; NADA, *N*-arachidonoyl dopamine; PMSF, phenylmethylsulfonyl fluoride; $TRPV_1$, transient release potential family vanilloid type-1; VGCC, voltage-gated Ca^{2+} channel

Introduction

A group of endogenous arachidonic acid derivatives, such as arachidonoylethanolamide (anandamide, AEA) and *N*-arachidonoyl dopamine (NADA), can activate both the cannabinoid type-1 receptor (CB_1) (Devane *et al*., 1992; Bisogno *et al*., 2000) and the transient release potential family vanilloid type-1 ($TRPV_1$) vanilloid receptor (van der Stelt and Di Marzo, 2004; Bradshaw and Walker, 2005). These substances are therefore called hybrid endocannabinoid/endovanilloid ligands.

The predominant neuronal cannabinoid receptor, the CB_1 receptor, is involved in several (patho)physiological mechanisms in the hippocampus. These include, for instance, modulation of spatial and short-term memory, seizure threshold or β-amyloid-induced pathophysiological changes (Lichtman and Martin, 1996; Mallet and Beninger, 1998; Wallace *et al*., 2002; Chen *et al*., 2003; Mazzola *et al*., 2003; Piomelli, 2003; Ramirez *et al*., 2005). The widespread functional presence of CB_1 receptors in nerve terminals of the hippocampus has been well documented (Katona *et al*., 1999; Degroot *et al*., 2006; Kawamura *et al*., 2006). Activation

Correspondence: Dr A Köfalvi, Faculty of Medicine, Center for Neurosciences of Coimbra, Institute of Biochemistry, University of Coimbra, 1 Rua Larga, Coimbra 3004-504, Portugal.
E-mail: akofalvi@yahoo.com
[3]Current address: Instituto de Neurociencias de Alicante, CSIC-UMH (Lab 202) Apartado 18; 03550 San Juan de Alicante, Alicante, Spain.
Received 30 October 2006; revised 25 January 2007; accepted 12 February 2007; published online 16 April 2007

of the CB_1 receptor by its first discovered endogenous agonist AEA (Devane *et al*., 1992) and the recently discovered NADA (Bisogno *et al*., 2000) can induce a great diversity of intracellular responses, including the inhibition of Ca^{2+} channel opening which decreases transmitter release (Howlett *et al*., 2004).

$TRPV_1$ receptors are assumed to be present in the hippocampal neurons (Mezey *et al*., 2000; Roberts *et al*., 2004; Toth *et al*., 2005). Activation of the $TRPV_1$ receptor causes Ca^{2+} and Na^+ entry and neuronal depolarization. Interestingly, only a few *ex vivo* studies have demonstrated a presumably presynaptic site of action for $TRPV_1$ receptors in the hippocampus. For instance, AEA and NADA were shown to increase paired-pulse depression, in a manner sensitive to $TRPV_1$ receptor antagonists (Al-Hayani *et al*., 2001; Huang *et al*., 2002). This implies that the predominant effect of hybrid agonists might be excitation by presynaptic $TRPV_1$ receptor activation rather than inhibition by presynaptic CB_1 receptor activation. However, the predominant location of the $TRPV_1$ receptor, determined with immunohistochemistry, is more likely to be postsynaptic in the hippocampus (Toth *et al*., 2005; Cristino *et al*., 2006). This conclusion is strengthened by the observation that selective and potent agonists of the $TRPV_1$ receptor, such as capsaicin and resiniferatoxin, failed to induce Ca^{2+} entry and γ-aminobutyric acid (GABA) release in hippocampal nerve terminals (Köfalvi *et al*., 2006). Instead, *E*- and *Z*-capsaicin, and the $TRPV_1$ receptor antagonist iodoresiniferatoxin as well as the CB_1 receptor antagonist AM251 concentration-dependently inhibited the high K^+-induced Ca^{2+} entry and GABA release in hippocampal nerve terminals. Furthermore, iodoresiniferatoxin shifted the concentration–response curve of AM251 to the right but did not affect the size of maximal inhibition. These findings point toward a common site of action, such that ligands for the CB_1 receptor and the $TRPV_1$ receptor can directly modulate intracellular Ca^{2+} levels ($[Ca^{2+}]_i$) via blocking voltage-gated Ca^{2+} channels (VGCCs).

These all are in agreement with the general notion that endocannabinoid and endovanilloid substances have additional targets (new putative receptors, ion channels) both in the hippocampus and in other brain areas (Pertwee, 2004; van der Stelt and Di Marzo, 2005; Oz, 2006). For instance, we have shown earlier that cannabinoid ligands are able to inhibit the release of glutamate, evoked with a strong stimulation by high K^+, in the hippocampus and in the striatum, via CB_1 receptor-independent mechanisms (Köfalvi *et al*., 2003, 2005). However, this should not undermine the role of presynaptic CB_1 receptors in the control of excitatory synaptic transmission, which was recently emphasized by different groups (Kawamura *et al*., 2006; Takahashi and Castillo, 2006).

There are many possible mechanisms by which cannabinoid and vanilloid receptor ligands may affect membrane excitability and $[Ca^{2+}]_i$, and, concomitantly, neural transmission and cell injury. Therefore, careful studies are required to understand the ill-defined mechanisms of action of hybrid endocannabinoid/endovanilloid agonists. Our main goal here was to explore how hybrid endocannabinoid/endovanilloid ligands affect resting and stimulated $[Ca^{2+}]_i$ levels and [^{3}H]amino acid release in hippocampal nerve terminals from rat brain.

Methods

Preparation of synaptosomes

All studies were conducted in accordance with the principles and procedures outlined in the EU guidelines and were approved by the local Animal Care Committee of the Institute. All efforts were made to reduce the number of animals used and to minimize their suffering. Male Wistar rats, 140–160 g; Charles-River, Barcelona, Spain) were anesthetized with halothane before being decapitated.

For fluorimetric assay. A synaptosomal fraction of the hippocampi was prepared with slight modifications of the technique described by Köfalvi *et al*. (2006). For each experiment, hippocampi from two rats were quickly removed into ice-cold sucrose solution (0.32 M, containing 5 mM 4-(2-hydroxyethyl)-1-piperazineethanesulfonic acid (HEPES), pH 7.4) and were homogenized instantly with a Teflon homogenizer and centrifuged at 2000 *g* for 3 min. The supernatant was centrifuged at 13 000 *g* for 12 min. The mitochondria-free fraction of the pellet was collected and washed at 13 000 *g* for 2 min in sucrose solution at 4°C, then decanted and stored in a sealed container on ice.

For [^{3}H]GABA and [^{3}H]glutamate release assay. As described earlier (Köfalvi *et al*., 2005), the removed hippocampi were rapidly dissected and were homogenized in ice-cold 0.32 M sucrose solution (containing 1 mM EDTA, 1 mg/ml bovine serum albumin and 5 mM HEPES, pH 7.4) at 4°C and centrifuged at 2000 *g* for 10 min. The supernatant was centrifuged at 13 000 *g* for 12 min. The pellet was resuspended in ice-cold 45% (v/v) Percoll in Krebs solution (pH 7.4) and centrifuged at 13 000 *g* for 2 min to eliminate free mitochondria and glial debris. The top layer was washed twice at 13 000 *g* at 4°C for 2 min in oxygenated Krebs solution of the following composition (in mM): NaCl 113, KCl 3, KH_2PO_4 1.2, $MgSO_4$ 1.2, $CaCl_2$ 2.5, $NaHCO_3$ 25, glucose 10, oxygenated with 95% O_2 and 5% CO_2, pH 7.4.

Fluorimetric assay

Experiments were performed as described earlier (Köfalvi *et al*., 2006): synaptosomal pellets (1 mg protein) were preincubated with Fura2/AM (5 μM) for 20 min at 25°C in the incubation solution of the following composition: NaCl (132 mM), KCl (1 mM), $MgCl_2$ (1 mM), $CaCl_2$ (0.1 mM), H_3PO_4 (1.2 mM), glucose (10 mM), HEPES (10 mM) and pH 7.4. Then the pellet was centrifuged at 13 000 *g*, washed and resuspended in 2 ml assay solution (NaCl (132 mM), KCl (3.1 mM), $MgCl_2$ (1.2 mM), $CaCl_2$ (2.5 mM), H_3PO_4 (0.4 mM), glucose (10 mM), HEPES (10 mM), pH 7.4). The fluorescence was monitored at 37°C, using a computer-assisted Spex Industries (Edison, NJ, USA) Fluoromax spectrofluorometer at 510 nm emission and double excitation at 340 and 380 nm, using 5 nm slits. After the 4-min stabilization period (T_{-240}–T_0 s), data were collected at 2 s intervals. The first 90 s (45 data points; T_0–T_{90}) represented the pretreatment period, and then 2 μl of the stock drug solutions was applied. Two hundred and seventy seconds later (T_{360}), the synaptosomes were challenged with 20 μl of KCl solution

(final concentration of 20 mM). The calibration was made using 5 μM ionomycin (R_{max}), at T_{400} and 5 mM ethylene glycol bis(β-aminoethylether)-*N,N,N′,N′*,-tetraacetic acid (EGTA)/30 mM Tris, pH 9.6 (R_{min}), at T_{500}. The fluorescence intensities were converted into $[Ca^{2+}]_i$ values by using the calibration equation for double excitation wavelength measurements and taking the dissociation constant of the Fura-2/Ca^{2+} complex as 224 nM (Grynkiewicz *et al*., 1985). In calcium-free experiments, the synaptosomal pellet was incubated at room temperature in the assay medium for 5 min to allow the saturation of the intracellular stores, and then was washed twice in an assay medium of similar composition but without addition of $CaCl_2$. All other steps were identical except that ionomycin was administered together with 5 μl of $CaCl_2$ (1 M, final concentration of 2.5 mM) to establish R_{max}. In acidification experiments, HEPES (7.5 mM) and methanesulfonic acid (MES) (7.5 mM) were used in the assay solution as a dual buffer providing useful buffer range up to pH 5.5. NaCl was decreased to 127 mM to maintain the same osmolarity. The pH in the cuvette was checked by a microtip pH meter.

Calculation

A predictive line was fitted to the first 45 data points with linear regression. Drug/vehicle effects were calculated as the change in $[Ca^{2+}]_i$ (nM) min^{-1}, compared with the predictive line (Figure 1b and c, dashed arrow) with the area under the curve method. The last 30 data points before KCl stimulation (T_{330}–T_{358}) were used to establish another predictive line. The maximal K^+-evoked Ca^{2+} entry between T_{360} and T_{374} was calculated as the greatest difference of the measured value from the extension of the latter predictive line. Every day, the first and the last synaptosomal samples were used to establish dimethylsulfoxide (DMSO) control values. Randomly, H_2O controls (2 μl H_2O into 2 ml assay volume, see Results section) were measured as an absolute control for DMSO (Figure 1d and e).

[^{3}H]GABA and [^{3}H]glutamate release assays from hippocampal synaptosomes

Experiments were performed with modifications of our previous studies (Köfalvi *et al*., 2003, 2005, 2006). The synaptosomes were diluted to 1 ml with Krebs solution, and equilibrated with careful oxygenation (95% O_2 and 5% CO_2) at 37°C for 5 min, and after that 10 μCi of [^{3}H]glutamate or [^{3}H]GABA (Amersham Pharmacia Biotech, Piscataway, NJ, USA) were added to the synaptosomes for 5 min. All solutions contained the GABA transaminase and glutamate decarboxylase inhibitor, aminooxyacetic acid (100 μM). Aliquots (70 μl, 500 μg protein) of the preloaded synaptosomes were transferred into 70 μl perfusion chambers, and were trapped between two layers of Whatman GF/C filters and superfused continuously at a rate of 0.7 ml/min until the end of the experiment. Upon termination of the 20-min washout, 2-min samples were collected for liquid scintillation assay. All experimental procedures were performed at 37°C. At the 6th and the 20th min of the sample collection period, release of transmitters was triggered twice (S_1 and S_2) with 20 mM K^+ (isomolar substitution of Na^+ by K^+ in the buffer) for 30 s. AEA and NADA were administered 10 min before S_2, whereas WIN55212-2 was given 2 min before S_2. The release of [^{3}H]GABA and [^{3}H]glutamate was entirely calcium-dependent: removal of Ca^{2+} combined with EGTA (1 mM) and the use of $CdCl_2$ (200 μM) diminished S_2 by 92.9% and 85.0%, respectively (Figure 5e and f). The proportion of GABA and glutamate in the released radioactivity was confirmed to be >95%, as reported previously (Köfalvi *et al*., 2005).

Data treatment

All data represent mean ± s.e.m. of $n \geqslant 6$ observations. Statistical significance was calculated by Student's *t*-test or analysis of variance followed by Bonferroni's test for selected pairs of columns, as appropriate, and $P < 0.05$ was accepted as showing a significant difference.

Drugs

NADA, EGTA, EDTA, HEPES, MES, Tris, DMSO, phenylmethylsulfonyl fluoride (PMSF), WIN55212-2, sucrose, aminooxyacetic acid, 2-aminoethoxydiphenyl borate (2APB), $ZnCl_2$, $GdCl_3$, epibatidine, sulpiride, fatty acid-free bovine serum albumin, halothane and ionomycin were obtained from Sigma (St Louis, MI, USA). AEA, SB366791, Ruthenium Red, AM630, AM251, JWH133 and DuP697 were obtained from Tocris Bioscience (Bristol, UK). Fura2/AM was purchased from Alfagene (Lisbon, Portugal). Non-water soluble substances were dissolved or reconstituted in DMSO, and aliquoted and stored at −20°C.

Up to the highest concentrations used, none of the tested compounds affected significantly the photometric measurements at the wavelengths used.

Results

Fluorimetric experiments

After the stabilization period, basal $[Ca^{2+}]_i$ at T_2 amounted to 90.2 ± 9.1 nM ($n = 13$, H_2O control). The 20 mM K^+-evoked $[Ca^{2+}]_i$ rise amounted to 245 ± 2.0 nM (2 μl H_2O control), which was not significantly modified by DMSO (0.1% v/v; 243 ± 2.4 nM, $n = 91$, $P > 0.05$; Figure 3a and b). DMSO increased the resting $[Ca^{2+}]_i$ (82.9 ± 18.6 nM min^{-1}) vs H_2O control (24.1 ± 21.0 nM min^{-1}, $P < 0.01$) (Figure 1a–e). However, using less than 2 μl of even more concentrated DMSO stock solutions would have had affected precision and drug solubility. As a positive drug control, epibatidine (100 nM; $n = 6$) was added at T_{90}, which caused a sustained $[Ca^{2+}]_i$ rise of 385.0 ± 43.2 nM min^{-1} ($P < 0.001$ vs DMSO alone; Figure 1a and d). Epibatidine failed to affect the K^+-evoked $[Ca^{2+}]_i$ entry (Figure 1a).

Endogenous CB_1/$TRPV_1$ ligands trigger an increase in resting $[Ca^{2+}]_i$

NADA (1–100 μM) triggered an immediate, sustained and concentration-dependent $[Ca^{2+}]_i$ rise. This effect of NADA

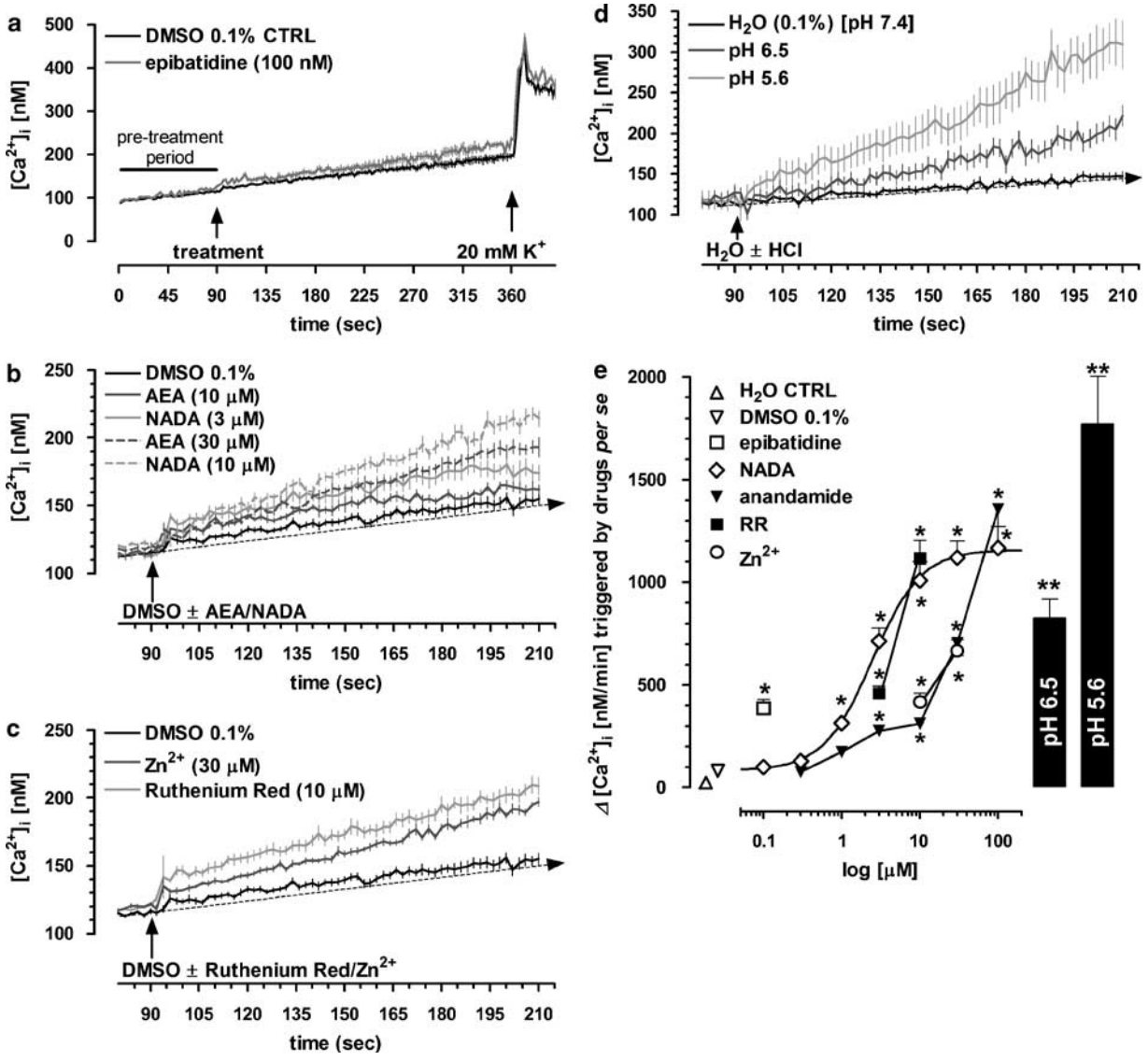

Figure 1 NADA, AEA, Ruthenium Red, Zn^{2+} and protons triggered a concentration-dependent $[Ca^{2+}]_i$ rise in rat hippocampal synaptosomes. (**a**) Averages of DMSO control experiments, and experiments with epibatidine (100 nM), as a validation for the technique. Fluorescence was monitored at 510 nm at 2 s intervals. After recording a baseline for 90 s (pre-treatment period, T_{90}), drug or vehicle was applied. At T_{360}, Ca^{2+} entry was stimulated with 20 mM K^+. (**b**) NADA and AEA, and (**c**) TASK-3 inhibitors, Ruthenium Red and Zn^{2+}, (all applied as indicated by the vertical arrows) trigger concentration-dependent rise of $[Ca^{2+}]_i$, and (**d**) lowering the pH of the buffer with 2 M HCl (as indicated by the vertical arrow) to 6.5 and 5.6 triggers rise of $[Ca^{2+}]_i$. All effects were compared with an extension of a line fitted with linear regression onto the values recorded during the pretreatment period. The dashed arrows in (**b**–**d**) represent such fitted lines for the DMSO and H_2O controls. Note that only 10 s are displayed from the pre-treatment period and 2 min after the treatment. (**e**) Concentration–response curves for the tested ligands. Black bars represent the size of the rise in $[Ca^{2+}]_i$ at different pH values and they share the same *Y*-axis as the concentration–response values. Values are represented as nM min^{-1} changes of $[Ca^{2+}]_i$ during the first 2 min after treatment. All data points are mean ± s.e.m. of $n \geqslant 6$ observations, $^*P < 0.05$ compared with H_2O or DMSO control.

reached a plateau around 30 μM, and displayed an EC_{50} of 2.4 μM (95% confidence interval: 2.19–2.73 μM; Figure 1b and e). AEA (3–100 μM) also triggered an immediate, sustained and concentration-dependent $[Ca^{2+}]_i$ rise. AEA was less potent and, up to 100 μM, did not reach a plateau effect (Figure 1b and e).

Blockade of metabolism does not counteract the $[Ca^{2+}]_i$ rise, triggered by NADA and AEA

Although the metabolic pathway for the catabolism of NADA is not yet established, AEA is believed to be metabolized into bioactive substances, such as arachidonic acid by the fatty acid aminohydrolase (FAAH) (McKinney and Cravatt, 2005), or prostaglandin E_2-type substances by cyclooxygenase-2 (COX-2) (Yu *et al*., 1997). In DDT_1 MF-2 smooth muscle cells, arachidonic acid activates a non-capacitive Ca^{2+} entry sensitive to Gd^{3+} (1 μM) (Demuth *et al*., 2005). Thus, the effect of NADA and AEA might be, at least partly, mediated by their possible metabolite, arachidonic acid. For this purpose, we tested AEA and NADA in the presence of either PMSF (300 μM), a non-specific irreversible amidase inhibitor that also inhibits the action of FAAH (Desarnaud *et al*., 1995), or DuP697 (100 nM), a selective

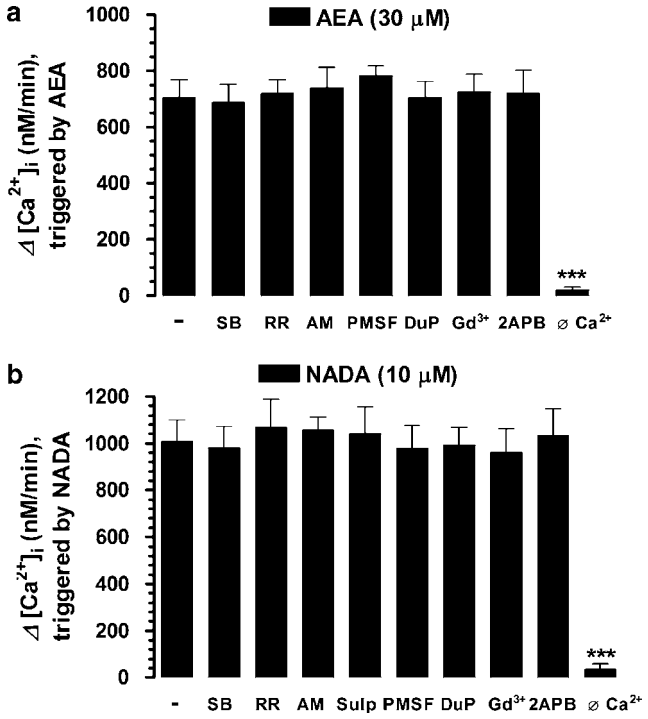

Figure 2 The AEA- (**a**) and NADA- (**b**) triggered rise in $[Ca^{2+}]_i$ was only prevented by the absence of external Ca^{2+}, but not by inhibitors of the $TRPV_1$, CB_1 or dopamine receptors, endocannabinoid-metabolizing enzymes FAAH and COX-2, the arachidonate-regulated non-capacitative Ca^{2+} entry and intracellular store-operated Ca^{2+} channels. Fluorimetric recordings were carried out as described in Figure 1. Antagonists and modulators (SB, SB366791; RR, Ruthenium Red; AM, AM251; Sulp, sulpiride; DuP, DuP697; 2APB, 2-aminoethoxydiphenyl borate; PMSF, phenylmethylsulfonyl fluoride; $\varnothing$ Ca^{2+}, Ca^{2+}-free) were applied at T_{-240}, that is 4 min before starting the recordings, and at T_{90}, either DMSO, or DMSO + AEA or NADA were applied. All data points are mean ± s.e.m. of $n \geqslant 6$ observations, ***$P < 0.001$, compared with respective controls of antagonists and modulators.

COX-2 inhibitor (Gans *et al*., 1990) or Gd^{3+} (1 μM) (all from T_{-240}). None of them counteracted either AEA- or NADA-triggered $[Ca^{2+}]_i$ rises ($n = 6$ in each case; Figure 2a and b) and none of them affected the basal $[Ca^{2+}]_i$ (data not shown).

The NADA- and AEA-triggered $[Ca^{2+}]_i$ rise depends on extracellular Ca^{2+}

2APB (3 μM), a complex inhibitor of intracellular store-operated Ca^{2+} release (Bootman *et al*., 2002) and modulator of TRPV receptor functions (Hu *et al*., 2004), applied from T_{-240}, also failed to modulate the $[Ca^{2+}]_i$ rise, triggered by AEA and NADA ($n = 6$ in each case; Figure 2a and b). In Ca^{2+}-free medium, neither NADA nor AEA were able to trigger any significant rise of resting $[Ca^{2+}]_i$ ($n = 6$ in each case; Figure 2a and b).

CB_1, CB_2 and $TRPV_1$ receptors are not involved in the $[Ca^{2+}]_i$ rise, triggered by NADA and AEA

As it was recently demonstrated that the peripheral type of cannabinoid receptor, the CB_2 receptor, may also have a function in brainstem neurons, we tested the potent mixed CB_1 receptor /CB_2 receptor agonist WIN55212-2 (100 nM), the selective CB_2 receptor agonist JWH133 (1 μM) (Huffman *et al*., 1999) as well as the selective CB_2 receptor antagonist AM630 (1 μM) (Mukherjee *et al*., 2004) on Ca^{2+} levels. None of them altered the basal $[Ca^{2+}]_i$ (applied from T_{-90}, data not shown). The selective CB_1 receptor antagonist AM251 has already been tested in a previous study (Köfalvi *et al*., 2006) and also failed to change the resting $[Ca^{2+}]_i$.

The general pore blocker and TRPV channel subfamily antagonist Ruthenium Red (3 μM) (Hu *et al*., 2004), and the selective $TRPV_1$ receptor antagonist SB366791 (3 μM) (Gunthorpe *et al*., 2004) as well as the CB_1 receptor antagonist AM251 (0.5 μM) (all from T_{-240}) failed to counteract the $[Ca^{2+}]_i$ rise, triggered by AEA (30 μM) and NADA (10 μM) ($n = 6$–8; Figure 2a and b).

TASK-3 inhibitors trigger the rise of resting $[Ca^{2+}]_i$ in a manner similar to that induced by AEA and NADA

In the previous subset of experiments, we observed that after the 4-min preincubation period with Ruthenium Red, $[Ca^{2+}]_i$ amounted to 203 ± 16 nM at T_2 ($n = 6$, $P < 0.001$ vs CTRL). In contrast, the other $TRPV_1$ receptor antagonist SB366791 failed to significantly alter $[Ca^{2+}]_i$ (99 ± 12 nM, $n = 6$, ns), indicating that the effect of Ruthenium Red is independent from $TRPV_1$ receptor blockade. Ruthenium Red and AEA in the micromolar range have been shown to directly block TASK-3 background potassium channels (Maingret *et al*., 2001; Czirjak and Enyedi, 2003) and thus depolarize neuronal membranes and trigger Ca^{2+} entry. To test this possibility in our system, we now applied Ruthenium Red (3 and 10 μM, $n = 6$) from T_{90} and found it to trigger a rapid, sustained, significant and concentration-dependent $[Ca^{2+}]_i$ rise, comparable to those induced by NADA and AEA (Figure 1c and e). Another inhibitor of TASK-3, Zn^{2+} (Clarke *et al*., 2004) at 10 and 30 μM, also triggered a rapid, sustained, significant and concentration-dependent $[Ca^{2+}]_i$ rise in our experiments (Figure 1c and e; $n = 6$).

TASK-3 channels are also inhibited by acidic pH (Kim *et al*., 2000; Czirjak and Enyedi, 2003; Aller *et al*., 2005). In our model, acidification triggered a sustained and significant $[Ca^{2+}]_i$ rise with similar kinetics to those observed upon the application of AEA, NADA, Ruthenium Red or Zn^{2+} (Figure 1d and e). At pH 6.5, the size of $[Ca^{2+}]_i$ rise was similar to that triggered by NADA at 3 μM and to that triggered by AEA at 30 μM. At pH 5.5, the $[Ca^{2+}]_i$ rise was slightly greater than that triggered by AEA at 100 μM, but this difference did not reach the level of statistical significance (Figure 1d and e).

CB_1 but not CB_2 receptors control the K^+-evoked Ca^{2+} entry in hippocampal nerve terminals

In this subset of experiments, we wanted to determine whether our experimental model was suitable to test CB_1 receptor-dependent mechanisms, such as inhibition of K^+-evoked Ca^{2+} entry. WIN55212-2 (100 nM, from T_{90}) inhibited the K^+-evoked Ca^{2+} entry, and this was fully abolished by the CB_1 receptor antagonist AM251 (500 nM) (Figure 3a and c). JWH133, up to the maximally CB_2 receptor-selective

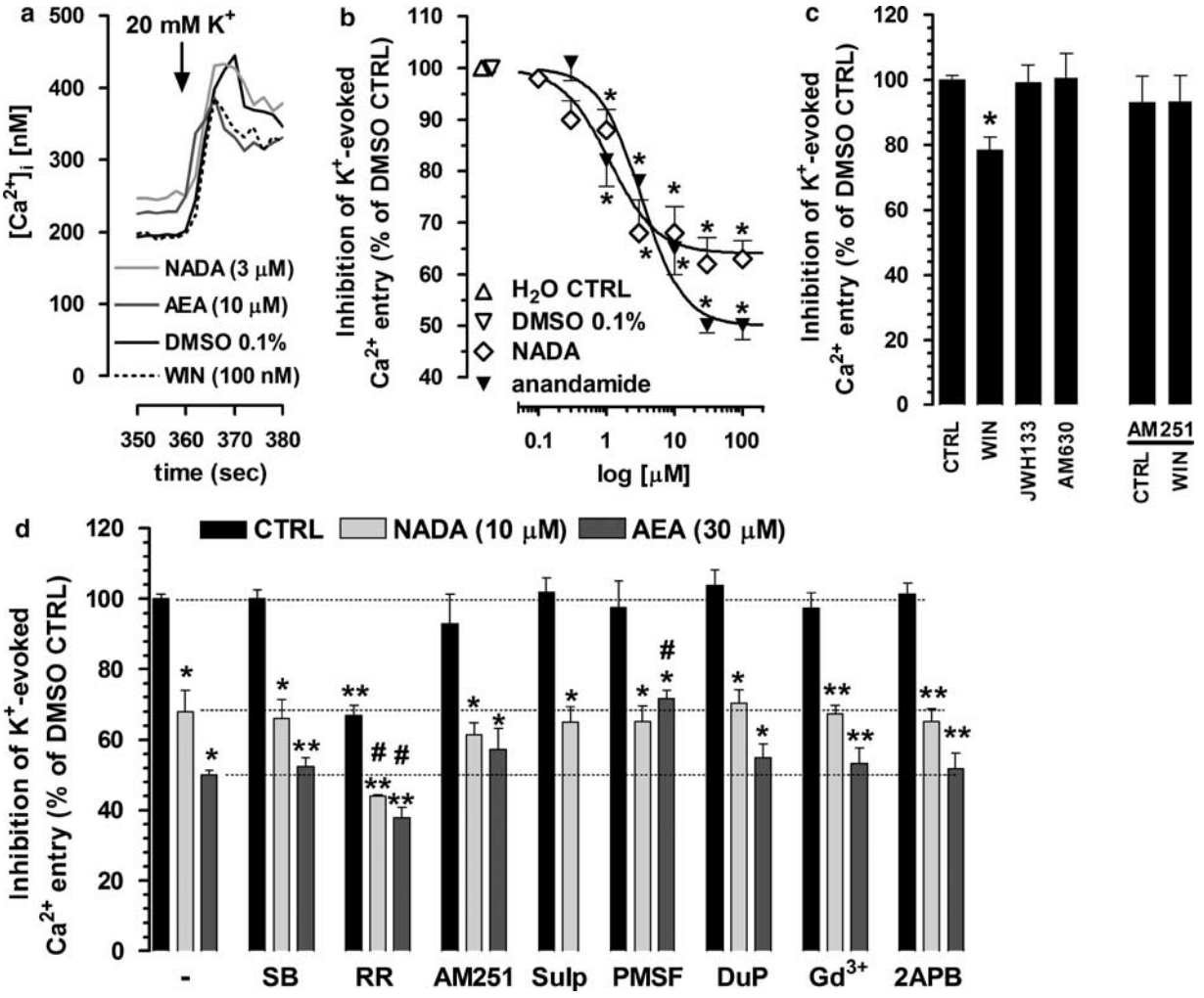

Figure 3 NADA and AEA concentration-dependently inhibited the K^+-evoked Ca^{2+} entry. (**a**) Representative traces of the K^+- (20 mM) evoked Ca^{2+} entry in the presence of vehicle (DMSO), NADA, AEA and WIN55212-2. Note that error bars are not displayed for the sake of clarity, and s.e.m. did not exceed 8% for any data point. (**b**) Concentration–response curves for AEA and NADA. (**c**) WIN55212-2 (WIN, 100 nM) also inhibited the K^+-evoked Ca^{2+} entry and this was antagonized by AM251 (500 nM). The CB_2 receptor-selective agonist JWH133 (1 μM) and the CB_2 receptor-selective antagonist AM630 (1 μM) failed to alter the K^+-evoked Ca^{2+}. (**d**) Inhibitors of the $TRPV_1$ receptor (SB, SB366791, 3 μM and RR, Ruthenium Red, 3 μM); CB_1 receptor (AM, AM251, 500 nM); dopamine receptors (Sulp, sulpiride, 3 μM) endocannabinoid-metabolizing enzymes FAAH (PMSF, phenylmethylsulfonyl fluoride, 100 μM) and COX-2 (DuP, DuP697, 100 nM); the arachidonate-regulated non-capacitative Ca^{2+}-entry (Gd^{3+}, 1 μM), and intracellular store-operated Ca^{2+} channels (2APB, 2-aminoethoxydiphenyl borate, 3 μM) failed to reverse the inhibition of NADA and AEA on the K^+-evoked Ca^{2+} entry. Note that the modification of NADA- and AEA-induced inhibition of the K^+-evoked Ca^{2+} entry was estimated by comparison to the respective controls, namely, DMSO + antagonist alone. All data points represent mean ± s.e.m. of $n \geqslant 6$ observations. $^*P<0.05$ and $^{**}P<0.01$ vs respective control. $^{\#}P<0.05$; it indicates that the extent of inhibition is significantly different in the absence vs in the presence of the antagonist.

concentration of 1 μM, failed to alter the K^+-evoked Ca^{2+} entry (Figure 3a and c). To exclude the possibility that any CB_2 receptors in our system were already under tonic activation, we tested the CB_2 receptor-selective antagonist AM630 (1 μM), which also failed to alter the K^+-evoked Ca^{2+} entry (Figure 3a and c).

The effect of CB_1/$TRPV_1$ ligands on the K^+-evoked Ca^{2+} entry

Besides triggering $[Ca^{2+}]_i$ entry *per se*, NADA and AEA concentration-dependently inhibited the subsequent K^+-evoked Ca^{2+} entry in the same experiment (Figure 3a, b and d). AEA was more effective but slightly less potent than NADA ($E_{max\ AEA}$ 50.0 ± 1.2%, $n=9$ vs $E_{max\ NADA}$ 38.0 ± 5.2%, $n=11$, $P<0.01$; and $EC_{50\ AEA}$ 3.2 μM, 95% confidence interval: 1.3–5.2 μM vs $EC_{50\ NADA}$ 1.1 μM, 0.6–2.0 μM).

CB_1, $TRPV_1$ or dopamine receptors are not involved in the inhibitory action of NADA and AEA

The inhibitory action of NADA and AEA might reasonably be mediated via activation of presynaptic CB_1 receptors. However, the CB_1 receptor antagonist AM251 (500 nM; from T_{-240}) failed to prevent the inhibition of K^+-evoked Ca^{2+} entry by AEA and NADA (Figure 3d). Higher concentrations of AM251 could not be tested since this AM251 is also a VGCC inhibitor with an IC_{50} of 1.1 μM (Köfalvi *et al*., 2006).

Among the antagonists of the $TRPV_1$ receptors SB366791 (3 μM, T_{-240}) *per se* had no effect on the evoked Ca^{2+} entry, whereas Ruthenium Red (3 μM, from T_{-240}) inhibited it by 35% (Figure 3d), perhaps reflecting this compound's blockade of VGCC (Tapia and Velasco, 1997). When Ruthenium Red was applied from T_{90}, it inhibited the K^+-evoked Ca^{2+} entry by 39.3% at 3 μM, and by 48.6% at 10 μM ($n=6$ and $P<0.01$ for each).

SB366791 (3 μM) did not significantly alter the percentage of inhibition exerted by NADA and AEA ($n=6$ for each). Ruthenium Red also failed to prevent the inhibition caused by AEA and NADA (Figure 3d). Moreover, Ruthenium Red did not add to the inhibition by AEA or NADA, even though it inhibited Ca^{2+} entry by itself (see above).

Another possibility was that the effect of NADA was mediated by the activation of inhibitory dopamine receptors by its possible metabolite, dopamine. However, sulpiride (from T_{-240}) at 3 μM, which concentration is enough to block D_2, D_3 and D_4 receptors, failed to prevent the inhibition of K^+-evoked Ca^{2+} entry ($n=6$; Figure 3d) as well as the NADA-evoked Ca^{2+} entry (Figure 2b). Sulpiride had no effect either on the K^+-evoked Ca^{2+} entry ($n=6$; Figure 3d) or on the resting $[Ca^{2+}]_i$ (data not shown). On the other hand, the FAAH inhibitor PMSF halved the extent of inhibition by AEA (from 50.0 to 26.4%, $P<0.05$), but not that of NADA (from 32.0 to 33.2%, ns; Figure 3d), compared with the PMSF control. DuP697, Gd^{3+} or 2APB did not significantly affect the K^+-evoked Ca^{2+} entry or the inhibitory action of NADA and AEA.

CB_1, but not CB_2 receptors, control the K^+-evoked release [^{3}H]GABA and [^{3}H]glutamate

As there is a strong link between $[Ca^{2+}]_i$ rise in the nerve terminals and the Ca^{2+}-dependent release of neurotransmitters, we tested the effects of the cannabinoid and vanilloid ligands and TASK-3 inhibitors, described above in a Ca^{2+}-dependent release model of preloaded [^{3}H]GABA and [^{3}H]glutamate in nerve terminals, isolated from the rat hippocampus. The basal release of [^{3}H]GABA in the first collected sample amounted to 2.14 ± 0.09 fractional release % (FR%) ($n=32$, control) and the basal release of [^{3}H]glutamate amounted to 3.35 ± 0.05 FR% ($n=36$, control). DMSO (as a vehicle control at 0.001% for NADA and AEA), introduced after the first 20 mM K^+ depolarization (S_1), did not affect the second K^+ depolarization-evoked releases (S_2), resulting in an S_2/S_1 ratio of 1.06 ± 0.03 for GABA and 0.96 ± 0.05 for glutamate (Figure 4a–d and 5a, b, e, and f). Omission of Ca^{2+} after S_1, combined with EGTA (1 mM) and Cd^{2+} ($CdCl_2$, 200 μM), abolished S_2 in case of both transmitters ($n=6$), indicating that the K^+-evoked releases were predominantly Ca^{2+}-dependent (Figure 5e and f).

The potent CB_1 receptor/CB_2 receptor agonist WIN55212-2 (10 nM–10 μM) inhibited the evoked release of [^{3}H]GABA and [^{3}H]glutamate in a concentration-dependent and biphasic fashion, leaving the resting release of the transmitters unaffected. In case of GABA, a plateau effect was observed up to 1 μM WIN55212-2 and, above 1 μM, a second phase of inhibition was detected (Figure 4c). AM251 (500 nM) fully antagonized the effect of WIN55212-2 (100 nM–1 μM), but failed to affect the inhibitory effect of higher concentrations of WIN55212-2 (Figure 4c). For glutamate, the plateau effect was observed up to 3 μM of WIN55212-2 and a second phase of inhibition appeared at concentrations of WIN55212-2 above 3 μM (Figure 4d). Again, AM251 (500 nM) fully antagonized the inhibition by WIN55212-2 up to 3 μM of the agonist but not the second phase of inhibition caused by higher concentrations of WIN55212-2 (Figure 4d).

As concentrations higher than 500 nM of the competitive antagonist AM251 might be required to counteract the effect of WIN55212-2 in the micromolar range, we tested AM251 at 5 μM against 10 μM WIN55212-2 (since 0.5 μM AM251 abolished the inhibitory action of 1 μM WIN55212-2). We know that AM251 inhibits Ca^{2+} entry and transmitter releases in the hippocampus and striatum with IC_{50} values of 1–3 μM (Köfalvi *et al*., 2003, 2005, 2006). In the present experiments, AM251 (5 μM) inhibited the first K^+ depolarization-evoked release of [^{3}H]GABA by 52% and of [^{3}H]glutamate by 38%. However, WIN55212-2 (10 μM), introduced before S_2, caused the same extent of inhibition on the second K^+ depolarization-evoked release of [^{3}H]GABA and of [^{3}H]glutamate (Figure 4e and f). Altogether, these findings indicate that the effect of WIN55212-2 in the micromolar range is CB_1 receptor-independent, and is likely to be owing to direct VGCC blockade (Shen and Thayer, 1998). Therefore, we determined the EC_{50} values for WIN55212-2 by choosing the maximum selective concentrations as 1 μM for GABA release (EC_{50}, 59.8 nM; 95% confidence interval: 51.2–67.4 nM) and 3 μM for glutamate release (EC_{50}, 63.1 nM; 42.5–91.1 nM; Figure 4a–d).

JWH133 (1 μM) failed to alter either the resting or the K^+ depolarization-evoked release of [^{3}H]GABA or of [^{3}H]glutamate (data not shown), indicating that the CB_2 receptor did not play a role in presynaptic regulation of transmitter release in our model.

Effects of NADA and AEA on the release [^{3}H]GABA and [^{3}H]glutamate are similar to those on the levels of $[Ca^{2+}]_i$

NADA (30 μM, $n=12$) and AEA (30 μM, $n=12$), introduced after S_1, triggered a sustained outflow of [^{3}H]GABA and [^{3}H]glutamate (Figure 5a–d). NADA was more effective at the same concentration, in agreement with its observed greater efficacy to trigger a rise in $[Ca^{2+}]_i$. The outflow of [^{3}H]GABA and [^{3}H]glutamate, triggered by NADA and AEA was not sensitive to the combined presence of SB366791 (3 μM) and AM251 (500 nM), both introduced from the beginning of the 20-min washout period. However, it was abolished when Ca^{2+} was omitted from the Krebs solution after S_1, combined with EGTA (1 mM) and Cd^{2+} ($CdCl_2$, 200 μM; Figure 5c and d). NADA attenuated the Ca^{2+}-dependent component (93%) of the K^+-evoked release of [^{3}H]GABA (S_2) by 27.9% ($P<0.05$ vs DMSO control) and that of [^{3}H]glutamate (85% Ca^{2+}-dependent component) by 48.4% ($P<0.001$; Figure 5e and f). AEA also attenuated the Ca^{2+}-dependent component of the K^+-evoked release of [^{3}H]GABA by 27.5% ($P<0.05$) and that of [^{3}H]glutamate by 87.5% ($P<0.001$; Figure 5e and f). The inhibitory action of NADA or AEA on the K^+-evoked release of transmitters was not modified by SB366791 and AM251 ($n=8$; Figure 5e

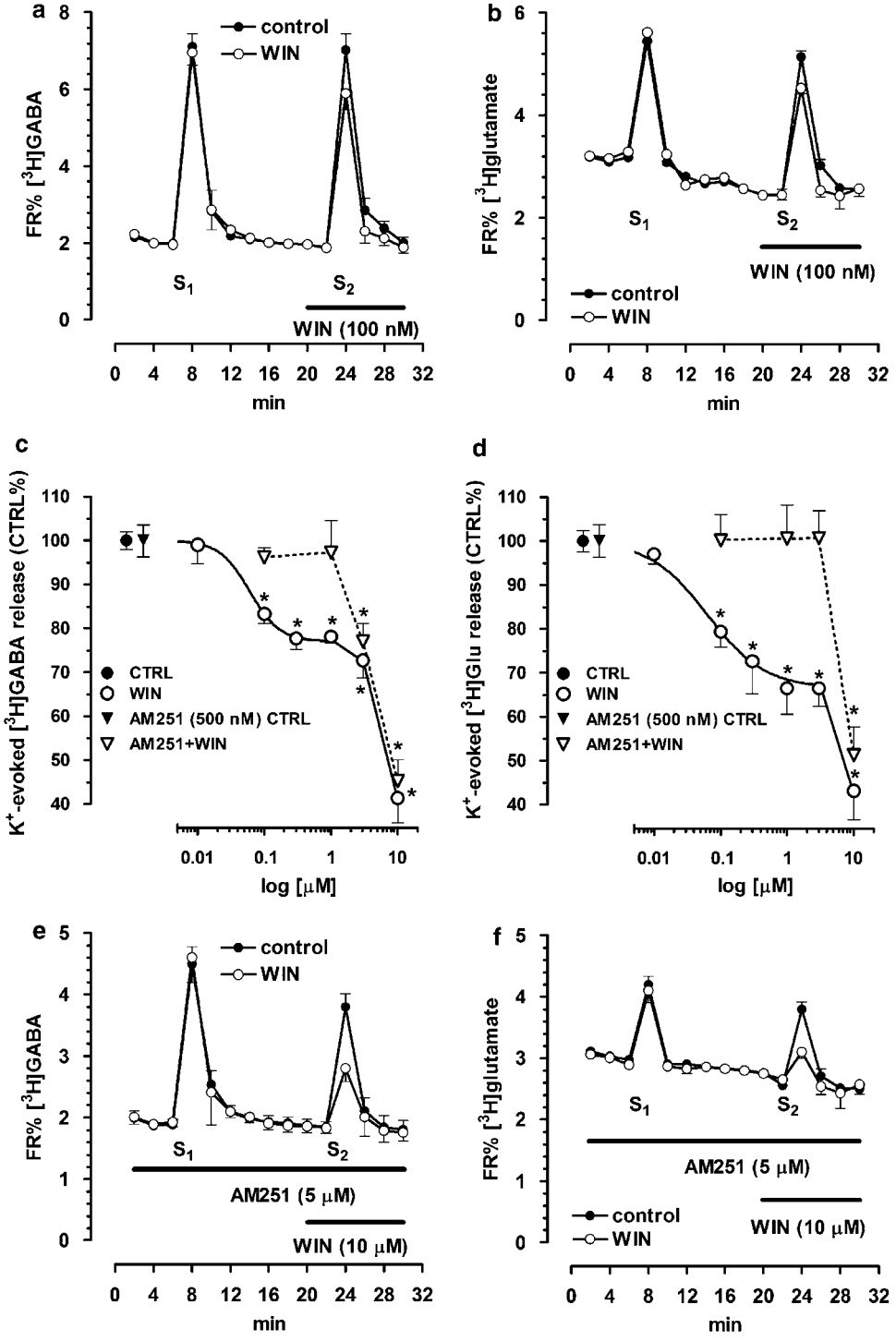

Figure 4 WIN55212-2 concentration-dependently inhibited the K^+-evoked release of [^{3}H]GABA and [^{3}H]glutamate from rat hippocampal synaptosomes via CB_1 receptor activation and direct Ca^{2+} channel blockade. (**a** and **b**) Synaptosomes were labeled either with [^{3}H]GABA (**a**) or [^{3}H]glutamate (**b**), and after 20 min of washout, 2-min samples were collected and counted for tritium, which is expressed as fractional release % (FR%). The synaptosomes were stimulated twice with 20 mM K^+, as indicated by S_1 and S_2. WIN55212-2 (WIN) and AM251 (500 nM) were applied as indicated by the horizontal bar. (**c** and **d**) Concentration–response curves for WIN55212-2 in the absence and in the presence of AM251 (500 nM). S_2/S_1 values of controls were taken as 100%. Note that the curves were fitted only to those concentrations of WIN55212-2, which displayed no significant difference from control in the presence of AM251. (**e** and **f**) AM251 even at the concentration of 5 μM, failed to counteract the inhibition by WIN55212-2 (10 μM) of the evoked release of [^{3}H]GABA (**e**) and [^{3}H]glutamate (**f**). Note that the scale of the *y*-axis is lower in **e** and **f**, in the presence of AM251 (5 μM), compared with its absence (see **a** and **b**), reflecting inhibition of Ca^{2+} entry by AM251, which is reflected by a lower K^+-evoked release of both transmitters. All data points represent mean$\pm$s.e.m. of $n=12$, $^*P<0.05$, compared with control (CTRL).

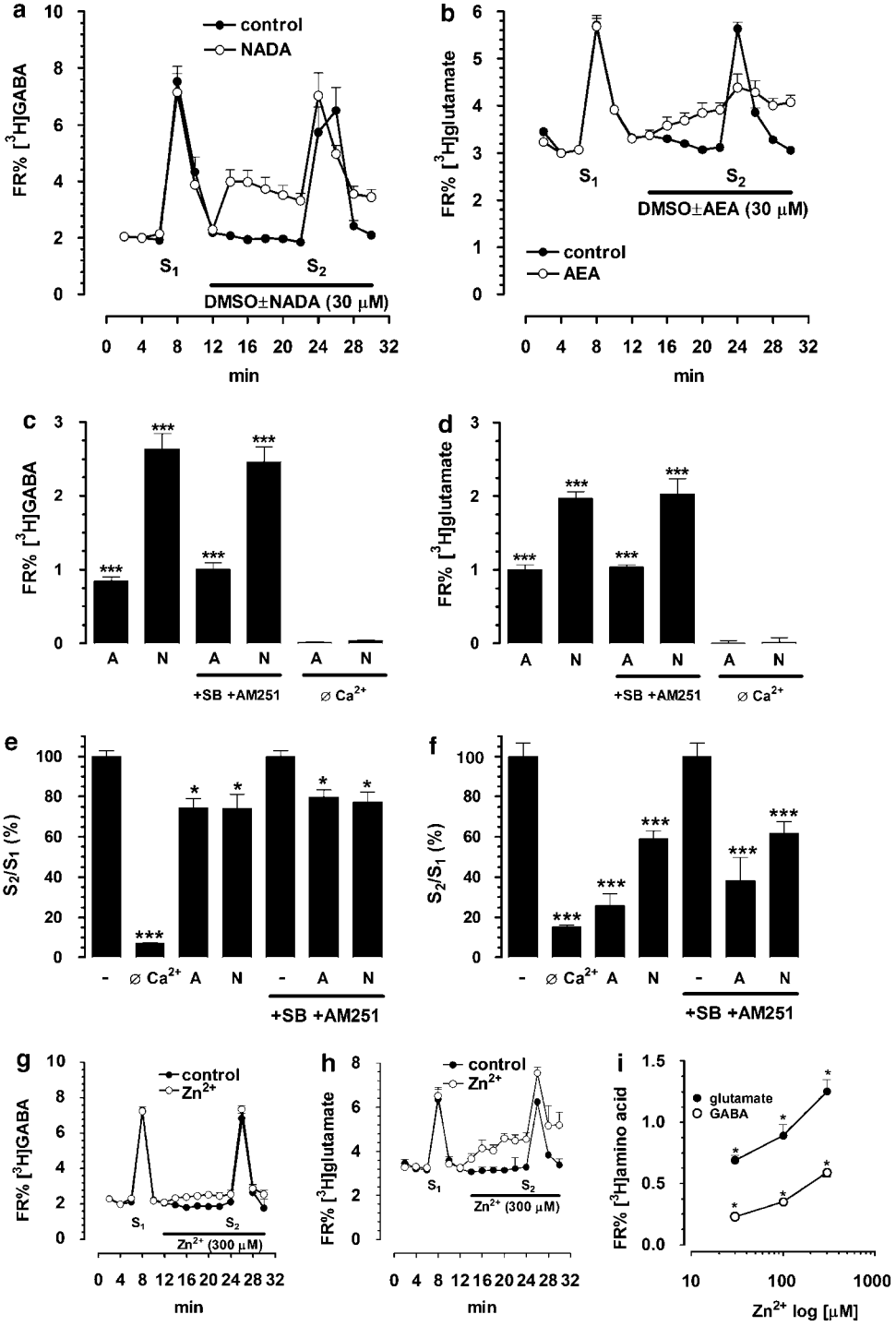

Figure 5 NADA, AEA and the TASK-3 inhibitor Zn^{2+} triggered *per se* the release of [^{3}H]GABA and [^{3}H]glutamate from hippocampal synaptosomes, and NADA and AEA, but not Zn^{2+}, also inhibited the subsequent K^+-evoked release of each transmitter. (**a** and **b**) Selected representative averages of time course experiments illustrating the effect of NADA on the release of [^{3}H]GABA (**a**) and of AEA on the release of [^{3}H]glutamate (**b**). NADA (30 μM) and AEA (30 μM) were applied as indicated by the horizontal bar. (**c** and **d**) Comparison of the amplitude of the release of [^{3}H]GABA and [^{3}H]glutamate, triggered by NADA [N] and AEA [A] alone, and in the presence of the $TRPV_1$ receptor antagonist SB366791 (SB, 3 μM) and the CB_1 receptor antagonist AM251 (AM, 500 nM). (**e** and **f**) Comparison of the inhibition of the K^+-evoked release of [^{3}H]GABA and [^{3}H]glutamate by NADA [N] and AEA [A] alone, and in the presence of the $TRPV_1$ receptor antagonist SB366791 (SB, 3 μM) and the CB_1 receptor antagonist AM251 (AM, 500 nM), or in Ca^{2+}-free medium ($\varnothing$ Ca^{2+} introduced after S_1 together with $CdCl_2$ and EGTA). In panels **c**–**f**, the antagonists were present from the beginning of the washout period onwards. (**g**–**i**) Zn^{2+} concentration-dependently triggered [^{3}H]GABA and [^{3}H]glutamate release *per se*, but did not affect the K^+-evoked release of each transmitter. All data points represent mean$\pm$s.e.m. of $n\geqslant 8$ observations. *$P<0.05$ and ***$P<0.001$.

and f). These observations in the transmitter release experiments are in parallel with effects of NADA and AEA in the Ca^{2+} measurement study.

The TASK-3 inhibitor Zn^{2+}, introduced after S_1, also triggered a concentration-dependent and sustained outflow of [^{3}H]GABA and [^{3}H]glutamate, similar to those triggered by AEA or NADA, but did not affect the K^+-evoked release of the transmitters (Figure 5g–i).

Discussion

Using our well-established pharmacological tools for the direct study of presynaptic neuromodulation (Katona *et al*., 1999; Köfalvi *et al*., 2003, 2005, 2006), we have demonstrated for the first time that NADA and AEA induced a rise of resting presynaptic $[Ca^{2+}]_i$, thus triggering the Ca^{2+}-dependent release of GABA and glutamate in hippocampal nerve terminals. Moreover, we show that NADA and AEA inhibited the K^+-evoked Ca^{2+} entry and the K^+-evoked Ca^{2+}-dependent release of GABA and glutamate.

NADA and AEA triggered $[Ca^{2+}]_i$ rise and release of GABA and glutamate, depending on the presence of external Ca^{2+}

A $[Ca^{2+}]_i$ rise, triggered by cannabinoid substances, is not without precedent in the hippocampus. For instance, cannabidiol, which is an antagonist at the CB_1 receptor and may have additional sites of action, elevates $[Ca^{2+}]_i$ by releasing Ca^{2+} from the intracellular stores (Drysdale *et al*., 2006). However, NADA and AEA triggered $[Ca^{2+}]_i$ rise via different mechanisms in our study, since 2APB, a complex inhibitor of Ca^{2+} release from intracellular stores (Bootman *et al*., 2002), failed to counteract the rise of basal $[Ca^{2+}]_i$. Furthermore, after allowing the replenishment of intracellular stores with Ca^{2+} and then removing Ca^{2+} from the external medium, NADA and AEA failed to trigger $[Ca^{2+}]_i$ rise and transmitter release. Altogether, these observations indicate that NADA and AEA caused entry of Ca^{2+} from the external medium, and we shall therefore refer to this effect as 'Ca^{2+} entry' rather than '$[Ca^{2+}]_i$ rise.'

As a previous study reported that NADA (50 μM) and micromolar 2APB caused sustained Ca^{2+} entry via $TRPV_1$ receptor activation in expression systems, which was sensitive to Ruthenium Red (3 μM) (Hu *et al*., 2004), we investigated this possibility in our system.

Cannabinoid, vanilloid and dopamine receptors and rapid metabolism were not involved in the observed effects of NADA and AEA

Endocannabinoid/endovanilloid ligands can induce Ca^{2+} entry through the $TRPV_1$ receptor (van der Stelt and Di Marzo, 2004). In our case, 2APB (which potentiates responses at the $TRPV_1$ receptor Hu *et al*., 2004), the $TRPV_1$ receptor antagonist SB366791 and the general TRPV receptor antagonist, Ruthenium Red, all failed to modulate the Ca^{2+} entry triggered by NADA and AEA. Accordingly, SB366791 also failed to antagonize transmitter release triggered by NADA and AEA. This indicates that ion channels, other than the TRP family channels, are involved in the observed effects of NADA and AEA. The reason for the virtual lack of $TRPV_1$ receptor function in hippocampal nerve terminals is detailed elsewhere (Köfalvi *et al*., 2006) and may be a consequence of the preferential post-synaptic location of the $TRPV_1$ receptor in the hippocampus (Toth *et al*., 2005; Cristino *et al*., 2006). Additionally, one can note that putative $TRPV_1$Rs in our system were not under an endogenous tone, as shown by the lack of effect of SB366791 *per se*.

Although NADA and AEA are partial agonists for the CB_1 receptor and the CB_2 receptor, the non-selective CB_1 receptor/CB_2 receptor agonist WIN55212-2 as well as the CB_2 receptor agonist JWH133 failed to modulate the resting $[Ca^{2+}]_i$, indicating that the effect of AEA and NADA were not mediated by these receptors.

NADA and AEA immediately triggered Ca^{2+} entry and this absence of lag in their effect argues against the involvement of a metabolic step. The lack of modulation of the effects of AEA and NADA by inhibitors of FAAH and COX-2 provided further evidence that metabolism of these compounds was not relevant to their activity here.

The arachidonate-regulated Ca^{2+} current (I_{ARC})

Recently, a novel mechanism for arachidonic acid-evoked Ca^{2+} entry has been described. This, the so-called 'non-capacitative Ca^{2+} entry channel,' through which arachidonic acid mediates Ca^{2+} influx, has been described in different cell types (Mignen and Shuttleworth, 2000; Fiorio Pla and Munaron, 2001). However, a known inhibitor of I_{ARC}, Gd^{3+} (1 μM) (Demuth *et al*., 2005), also failed to prevent NADA and AEA from triggering Ca^{2+} entry. Therefore, we have concluded that the arachidonic acid derivatives NADA and AEA did not induce significant I_{ARC} in our model.

Blockade of TASK-3 K^+ channels as a plausible explanation for the underlying mechanism

TASK-1 and TASK-3 are background, two pore domain, outward K^+ channels, which maintain the resting membrane potential, and are expressed in neurons (Callahan *et al*., 2004; Aller *et al*., 2005). TASK-3 is widely expressed in the hippocampus, whereas TASK-1 displays a restricted expression in the brain (Kim *et al*., 2000; Aller *et al*., 2005). Their functional relevance is illustrated by the ability of halothane to potentiate TASK currents, leading to hyperpolarization of neurons, which contributes to its general anesthetic action. A recent study has demonstrated that AEA in the low micromolar range fully blocks TASK-1 and partially inhibits TASK-3 channels (Maingret *et al*., 2001).

Assuming that AEA and its structural analogue NADA blocked TASK-1 and/or TASK-3 channels in our model, it is relatively easy to explain how the two ligands depolarized the plasma membrane and triggered Ca^{2+} entry. However, it is hard to directly test this hypothesis, since AEA and NADA are expected to function as channel blockers. Therefore, other modulators of TASK channels would fail to reverse their blockade. Our attempt to inhibit the AEA- and NADA-triggered Ca^{2+} entry with co-administration of halothane (9.4 mM) was not successful ($n = 3$ both for NADA and AEA,

data not shown). This is in agreement with the findings of Maingret *et al*. (2001), who showed that micromolar AEA almost completely abolished the millimolar halothane-induced outward currents.

We observed that AEA triggered small but already significant Ca^{2+} entry at 3 μM and the TASK-3 antagonist, Ruthenium Red (Czirjak and Enyedi, 2003) also elevated $[Ca^{2+}]_i$. These two findings point toward a possible involvement of TASK-3 rather than TASK-1. Zn^{2+} has been reported to be a less potent TASK-3 blocker than Ruthenium Red, developing its blockade over the micromolar concentration range (Clarke *et al*., 2004). In our study, Zn^{2+} also triggered Ca^{2+} entry and the release of the transmitters with efficacy and potency similar to those of the weak TASK-3 antagonist, AEA. Furthermore, WIN55212-2 has been shown to inhibit TASK-1, but not TASK-3 channels (Maingret *et al*., 2001) and, in our study, this substance was devoid of effect on the resting levels of Ca^{2+} and transmitter release. Assuming that both Ruthenium Red and AEA or NADA acted through TASK-3 channels, in the experiments summarized in Figure 2a and b, some modulation of each other's effects might have been expected. The lack of such interaction might be explained by the fact that none of the three drugs were tested at maximal concentrations and therefore the $[Ca^{2+}]_i$ in the presence of Ruthenium Red (3 μM) – taken as a baseline – still could have been surmounted with extra Ca^{2+} entry triggered by AEA or NADA.

An interesting functional similarity between the $TRPV_1$ receptor and the TASK-3 channel is that both interact with AEA, Ruthenium Red and protons. The net result of these interactions is expected to be membrane depolarization and Ca^{2+} entry. In fact, acidification has been demonstrated to inhibit TASK-3 channels (Kim *et al*., 2000; Czirjak and Enyedi, 2003; Aller *et al*., 2005) and, consequently, to inhibit hyperpolarizing leak K^+ conductance in cerebellar granule cells in culture (Lauritzen *et al*., 2003) and in thalamic relay neurons (Meuth *et al*., 2006). It is important to note that the TASK-1 channels were almost fully inhibited in the pH 7.4-6.5 ranges, whereas TASK-3 channels needed greater shift towards acidic pH to become fully blocked. As mentioned above, we could not demonstrate functional presynaptic hippocampal $TRPV_1$ receptors in the same pharmacological assays previously (Köfalvi *et al*., 2006), but we were able, in the present work, to show that acidification still triggered Ca^{2+} entry, suggesting that TASK type channels were functioning in our model. Further, our findings that acidification to pH 5.6 evoked twice as much Ca^{2+} entry as exposure to pH 6.5, indicated the involvement of TASK-3, rather than TASK-1 channels.

Altogether, TASK-3 channels are present in hippocampal neurons and their blockade is expected to depolarize membranes and trigger Ca^{2+} entry. In our model, known potent or weaker inhibitors of the TASK-3 channels, such as AEA, Ruthenium Red, Zn^{2+} and protons, all triggered similar Ca^{2+} entries, in concentration ranges described for the TASK-3 channels in expression models. Therefore, our data may suggest that the two chemically related hybrid endocannabinoid/endovanilloid substances AEA and NADA depolarize hippocampal nerve terminals via direct blockade of TASK-3 channels, thereby inducing Ca^{2+} entry and transmitter release. Further experiments in TASK-3 knockout mice could provide clear-cut evidence to support this hypothesis, once these animals are made available for public use. Until that time, the involvement of other targets cannot be excluded.

NADA and AEA inhibited the evoked Ca^{2+} entry and the evoked release of GABA and glutamate

In parallel with the findings on resting levels of Ca^{2+} and transmitters, we aimed to test the effect of cannabinoid, vanilloid and TASK-3 ligands on the K^+-evoked levels of Ca^{2+} and release of transmitters. We demonstrated that in the nanomolar range, WIN55212-2 inhibited K^+-evoked Ca^{2+} entry and K^+-evoked transmitter release in a CB_1 receptor-dependent fashion and also that CB_2 receptors did not control K^+-evoked Ca^{2+} entry and the release of transmitters. However, in the micromolar range, WIN55212-2 did inhibit the evoked release of GABA and glutamate in a CB_1 receptor-independent manner, very likely via direct VGCC blockade. This is in agreement with the findings of Shen and Thayer (1998), who proposed that WIN55212-2 directly blocks N- and P/Q-type VGCCs above 1 μM, thus masking the indirect, CB_1 receptor-mediated, inhibition of VGCCs. Furthermore, this resolves the apparent conflict on the release of glutamate between our previous data and those of Takahashi and Castillo (2006) and of Kawamura *et al*. (2006). Specifically, previously (Köfalvi *et al*., 2003, 2005) we used much longer (six times) stimulation with 30 mM K^+ to evoke glutamate release and this did not allow the observation of the CB_1 receptor-mediated modulation of release by WIN55212-2 in the nanomolar range. In the present series of experiments by using a more subtle, approximately 10-fold lower, stimulus which allows the detection of G protein-mediated presynaptic modulations (Ciruela *et al*., 2006), we were able to demonstrate that CB_1 receptors did control the release of glutamate and that the previously proposed CB_3 receptors are likely to correspond to actions exerted directly on VGCCs.

NADA and AEA are partial agonists of the CB_1 receptor and are much less potent than the full agonist WIN55212-2, but the maximal inhibitory effects (E_{max}) of NADA and AEA on the K^+-evoked responses were larger than the E_{max} of WIN55212-2 ($\leqslant$1 μM). Therefore, CB_1 receptors are unlikely to be solely involved in the inhibitory action of NADA and AEA. Accordingly, CB_1 receptor blockade failed to prevent the inhibitory actions of NADA and AEA on the K^+-evoked responses. The inhibition was also unaffected by the blockade of $TRPV_1$ receptors and dopamine receptors as well. AM251 alone also failed to modify the K^+-evoked Ca^{2+} entry, excluding the possibility that CB_1 receptors were under tonic activation during depolarization, which might have offset the CB_1 receptor-mediated effects of WIN55212-2, NADA and AEA.

Several ligands for the $TRPV_1$ receptor and CB_1 receptor have been shown to block voltage- and ligand-gated ion channels at low micromolar concentration. For instance, capsaicin, AEA, capsazepine, Ruthenium Red, AM404, AM251, SR141716A (Rimonabant) and WIN55212-2 block one or more of the Na^+, Ca^{2+}, K^+ channels as well

as 5-HT_3 and α7 nicotinic acetylcholine receptors (Shen and Thayer, 1998; White and Hiley, 1998; Kelley and Thayer, 2004; van der Stelt and Di Marzo, 2005; Köfalvi *et al*., 2006; Oz, 2006). In the present study, the high-efficacy agonist WIN55212-2 was able to inhibit transmitter release in the low nanomolar range via activation of CB_1 receptors, whereas the low affinity/partial agonist NADA and AEA might only activate CB_1 receptors in a higher concentration range in which they already directly block VGCCs as well.

Our finding that PMSF halved the inhibitory effect of AEA, suggested that a metabolite of AEA, generated by FAAH, also contributed to the inhibitory effect of AEA. Such effects could not be observed for NADA because NADA is also a FAAH inhibitor by itself (Bisogno *et al*., 2000). Our data also shed light on the mechanisms by which NADA and AEA affected the evoked release of GABA and glutamate with different potency. This could be because the different subtypes of VGCCs contributing to the depolarization-induced glutamate release were more sensitive to AEA and NADA than the VGCCs in GABAergic terminals.

Conclusions

For the first time with tools that allow the direct study of presynaptic mechanisms, we have demonstrated that AEA and NADA produced opposite effects on Ca^{2+} entry under depolarizing and non-depolarizing conditions. Furthermore, these effects may not necessarily result from the activation of $TRPV_1$ and CB_1 receptors. Further studies are required to understand the physiological and pathological significance of these findings. For instance, AEA has been shown to be neurotoxic and induce apoptosis of certain cells, but the underlying mechanisms are very complex and often controversial (Maccarrone and Finazzi-Agro, 2003). Presumably, AEA (and NADA) may kill a neuron simply with a massive depolarization if the cell expresses TASK-3. But the opposite is also possible: TASK-3 leak conductance has been shown to kill cerebellar granule cells; therefore, all compounds that block TASK-3 should prevent this type of cell death (Lauritzen *et al*., 2003). Both AEA and NADA can accumulate in excess under depolarizing pathological conditions, such as epilepsy and stroke, and they may either exacerbate or inhibit calcium entry and release of glutamate, providing excellent therapeutic targets.

Acknowledgements

This study was supported by the III/BIO/56/2005, and by the Fundação para a Ciência e Tecnologia (POCI2010/SFRH/BPD/18506/2004).

Conflict of interest

The authors state no conflict of interest.

References

Al-Hayani A, Wease KN, Ross RA, Pertwee RG, Davies SN (2001). The endogenous cannabinoid anandamide activates vanilloid receptors in the rat hippocampal slice. *Neuropharmacology* **41**: 1000–1005.

Aller MI, Veale EL, Linden AM, Sandu C, Schwaninger M, Evans LJ *et al*. (2005). Modifying the subunit composition of TASK channels alters the modulation of a leak conductance in cerebellar granule neurons. *J Neurosci* **25**: 11455–11467.

Bisogno T, Melck D, Bobrov MYu, Gretskaya NM, Bezuglov VV, De Petrocellis L *et al*. (2000). *N*-acyl-dopamines: novel synthetic CB_1 cannabinoid-receptor ligands and inhibitors of anandamide inactivation with cannabimimetic activity *in vitro* and *in vivo*. *Biochem J* **351**: 817–824.

Bootman MD, Collins TJ, Mackenzie L, Roderick HL, Berridge MJ, Peppiatt CM (2002). 2-aminoethoxydiphenyl borate (2-APB) is a reliable blocker of store-operated Ca^{2+} entry but an inconsistent inhibitor of $InsP_3$-induced Ca^{2+} release. *FASEB J* **16**: 1145–1150.

Bradshaw HB, Walker JM (2005). The expanding field of cannabimimetic and related lipid mediators. *Br J Pharmacol* **144**: 459–465.

Callahan R, Labunskiy DA, Logvinova A, Abdallah M, Liu C, Cotten JF *et al*. (2004). Immunolocalization of TASK-3 (KCNK9) to a subset of cortical neurons in the rat CNS. *Biochem Biophys Res Commun* **319**: 525–530.

Chen K, Ratzliff A, Hilgenberg L, Gulyas A, Freund TF, Smith M *et al*. (2003). Long-term plasticity of endocannabinoid signaling induced by developmental febrile seizures. *Neuron* **39**: 599–611.

Ciruela F, Casado V, Rodrigues RJ, Lujan R, Burgueno J, Canals M *et al*. (2006). Presynaptic control of striatal glutamatergic neurotransmission by adenosine A_1–A_{2A} receptor heteromers. *J Neurosci* **26**: 2080–2087.

Clarke CE, Veale EL, Green PJ, Meadows HJ, Mathie A (2004). Selective block of the human 2-P domain potassium channel, TASK-3, and the native leak potassium current, IKSO, by zinc. *J Physiol* **560**: 51–62.

Cristino L, de Petrocellis L, Pryce G, Baker D, Guglielmotti V, Di Marzo V (2006). Immunohistochemical localization of cannabinoid type 1 and vanilloid transient receptor potential vanilloid type 1 receptors in the mouse brain. *Neuroscience* **139**: 1405–1415.

Czirjak G, Enyedi P (2003). Ruthenium red inhibits TASK-3 potassium channel by interconnecting glutamate 70 of the two subunits. *Mol Pharmacol* **63**: 646–652.

Degroot A, Köfalvi A, Wade MR, Davis RJ, Rodrigues RJ, Rebola N *et al*. (2006). CB_1 receptor antagonism increases hippocampal acetylcholine release: site and mechanism of action. *Mol Pharmacol* **70**: 1236–1245.

Demuth DG, Gkoumassi E, Droge MJ, Dekkers BG, Esselink HJ, van Ree RM *et al*. (2005). Arachidonic acid mediates non-capacitative calcium entry evoked by CB_1-cannabinoid receptor activation in DDT1 MF-2 smooth muscle cells. *J Cell Physiol* **205**: 58–67.

Desarnaud F, Cadas H, Piomelli D (1995). Anandamide amidohydrolase activity in rat brain microsomes. Identification and partial characterization. *J Biol Chem* **270**: 6030–6035.

Devane WA, Hanus L, Breuer A, Pertwee RG, Stevenson LA, Griffin G *et al*. (1992). Isolation and structure of a brain constituent that binds to the cannabinoid receptor. *Science* **258**: 1946–1949.

Drysdale AJ, Ryan D, Pertwee RG, Platt B (2006). Cannabidiol-induced intracellular Ca^{2+} elevations in hippocampal cells. *Neuropharmacology* **50**: 621–631.

Fiorio Pla A, Munaron L (2001). Calcium influx, arachidonic acid, and control of endothelial cell proliferation. *Cell Calcium* **30**: 235–244.

Gans KR, Galbraith W, Roman RJ, Haber SB, Kerr JS, Schmidt WK *et al*. (1990). Anti-inflammatory and safety profile of DuP 697, a novel orally effective prostaglandin synthesis inhibitor. *J Pharmacol Exp Ther* **254**: 180–187.

Grynkiewicz G, Poenie M, Tsien RY (1985). A new generation of Ca^{2+} indicators with greatly improved fluorescence properties. *J Biol Chem* **260**: 3440–3450.

Gunthorpe MJ, Rami HK, Jerman JC, Smart D, Gill CH, Soffin EM *et al*. (2004). Identification and characterisation of SB-366791, a potent and selective vanilloid receptor (VR_1/$TRPV_1$) antagonist. *Neuropharmacology* **46**: 133–149.

Howlett AC, Breivogel CS, Childers SR, Deadwyler SA, Hampson RE, Porrino LJ (2004). Cannabinoid physiology and pharmacology: 30 years of progress. *Neuropharmacology* **47**: 345–358.

Hu HZ, Gu Q, Wang C, Colton CK, Tang J, Kinoshita-Kawada M *et al*. (2004). 2-Aminoethoxydiphenyl borate is a common activator of $TRPV_1$, $TRPV_2$, and $TRPV_3$. *J Biol Chem* **279**: 35741–35748.

Huang SM, Bisogno T, Trevisani M, Al-Hayani A, De Petrocellis L, Fezza F *et al*. (2002). An endogenous capsaicin-like substance with high potency at recombinant and native vanilloid VR_1 receptors. *Proc Natl Acad Sci USA* **99**: 8400–8405.

Huffman JW, Liddle J, Yu S, Aung MM, Abood ME, Wiley JL *et al*. (1999). 3-(1′,1′-Dimethylbutyl)-1-deoxy-delta8-THC and related compounds: synthesis of selective ligands for the CB_2 receptor. *Bioorg Med Chem* **7**: 2905–2914.

Katona I, Sperlágh B, Sík A, Köfalvi A, Vizi ES, Mackie K *et al*. (1999). Presynaptically located CB_1 cannabinoid receptors regulate GABA release from axon terminals of specific hippocampal interneurons. *J Neurosci* **19**: 4544–4558.

Kawamura Y, Fukaya M, Maejima T, Yoshida T, Miura E, Watanabe M *et al*. (2006). The CB_1 cannabinoid receptor is the major cannabinoid receptor at excitatory presynaptic sites in the hippocampus and cerebellum. *J Neurosci* **26**: 2991–3001.

Kelley BG, Thayer SA (2004). Anandamide transport inhibitor AM404 and structurally related compounds inhibit synaptic transmission between rat hippocampal neurons in culture independent of cannabinoid CB_1 receptors. *Eur J Pharmacol* **496**: 33–39.

Kim Y, Bang H, Kim D (2000). TASK-3, a new member of the tandem pore K^+ channel family. *J Biol Chem* **275**: 9340–9347.

Köfalvi A, Oliveira CR, Cunha RA (2006). Lack of evidence for functional $TRPV_1$ vanilloid receptors in rat hippocampal nerve terminals. *Neurosci Lett* **403**: 151–156.

Köfalvi A, Rodrigues RJ, Ledent C, Mackie K, Vizi ES, Cunha RA *et al*. (2005). Involvement of cannabinoid receptors in the regulation of neurotransmitter release in the rodent striatum: a combined immunochemical and pharmacological analysis. *J Neurosci* **25**: 2874–2884.

Köfalvi A, Vizi ES, Ledent C, Sperlágh B (2003). Cannabinoids inhibit the release of [^{3}H]glutamate from rodent hippocampal synaptosomes via a novel CB_1 receptor-independent action. *Eur J Neurosci* **18**: 1973–1978.

Lauritzen I, Zanzouri M, Honore E, Duprat F, Ehrengruber MU, Lazdunski M *et al*. (2003). K^+-dependent cerebellar granule neuron apoptosis. Role of task leak K^+ channels. *J Biol Chem* **278**: 32068–32076.

Lichtman AH, Martin BR (1996). Delta 9-tetrahydrocannabinol impairs spatial memory through a cannabinoid receptor mechanism. *Psychopharmacology (Berl)* **126**: 125–131.

Maccarrone M, Finazzi-Agro A (2003). The endocannabinoid system, anandamide and the regulation of mammalian cell apoptosis. *Cell Death Differ* **10**: 946–955.

Maingret F, Patel AJ, Lazdunski M, Honore E (2001). The endocannabinoid anandamide is a direct and selective blocker of the background K^+ channel TASK-1. *EMBO J* **20**: 47–54.

Mallet PE, Beninger RJ (1998). The cannabinoid CB_1 receptor antagonist SR141716A attenuates the memory impairment produced by delta9-tetrahydrocannabinol or anandamide. *Psychopharmacology (Berl)* **140**: 11–19.

Mazzola C, Micale V, Drago F (2003). Amnesia induced by beta-amyloid fragments is counteracted by cannabinoid CB_1 receptor blockade. *Eur J Pharmacol* **77**: 219–225.

McKinney MK, Cravatt BF (2005). Structure and function of fatty acid amide hydrolase. *Annu Rev Biochem* **74**: 411–432.

Meuth SG, Kanyshkova T, Meuth P, Landgraf P, Munsch T, Ludwig A *et al*. (2006). Membrane resting potential of thalamocortical relay neurons is shaped by the interaction among TASK3 and HCN2 channels. *J Neurophysiol* **96**: 1517–1529.

Mezey E, Toth Z.E, Cortright DN, Arzubi MK, Krause JE, Elde R *et al*. (2000). Distribution of mRNA for vanilloid receptor subtype 1 (VR_1), and VR_1-like immunoreactivity, in the central nervous system of the rat and human. *Proc Natl Acad Sci USA* **97**: 3655–3660.

Mignen O, Shuttleworth TJ (2000). I_{ARC}, a novel arachidonate-regulated, noncapacitative Ca^{2+} entry channel. *J Biol Chem* **275**: 9114–9119.

Mukherjee S, Adams M, Whiteaker K, Daza A, Kage A, Cassar S *et al*., (2004). Species comparison and pharmacological characterization of rat and human CB_2 cannabinoid receptors. *Eur J Pharmacol* **505**: 1–9.

Oz M (2006). Receptor-independent effects of endocannabinoids on ion channels. *Curr Pharm Des* **12**: 227–239.

Pertwee RG (2004). Novel pharmacological targets for cannabinoids. *Curr Neuropharm* **2**: 9–29.

Piomelli D (2003). The molecular logic of endocannabinoid signalling. *Nat Rev Neurosci* **4**: 873–884.

Ramirez BG, Blazquez C, Gomez del Pulgar T, Guzman M, de Ceballos ML (2005). Prevention of Alzheimer's disease pathology by cannabinoids: neuroprotection mediated by blockade of microglial activation. *J Neurosci* **25**: 1904–1913.

Roberts JC, Davis JB, Benham CD (2004). [^{3}H]Resiniferatoxin autoradiography in the CNS of wild-type and $TRPV_1$ null mice defines $TRPV_1$ ($VR\text{-}_1$) protein distribution. *Brain Res* **995**: 176–183.

Shen M, Thayer SA (1998). The cannabinoid agonist Win55,212-2 inhibits calcium channels by receptor-mediated and direct pathways in cultured rat hippocampal neurons. *Brain Res* **783**: 77–84.

Takahashi KA, Castillo PE (2006). The CB_1 cannabinoid receptor mediates glutamatergic synaptic suppression in the hippocampus. *Neuroscience* **139**: 795–802.

Tapia R, Velasco I (1997). Ruthenium red as a tool to study calcium channels, neuronal death and the function of neural pathways. *Neurochem Int* **30**: 137–147.

Toth A, Boczan J, Kedei N, Lizanecz E, Bagi Z, Papp Z *et al*. (2005). Expression and distribution of vanilloid receptor 1 ($TRPV_1$) in the adult rat brain. *Brain Res Mol Brain Res* **135**: 162–168.

van der Stelt M, Di Marzo V (2004). Endovanilloids. Putative endogenous ligands of transient receptor potential vanilloid 1 channels. *Eur J Biochem* **271**: 1827–1834.

van der Stelt M, Di Marzo V (2005). Anandamide as an intracellular messenger regulating ion channel activity. *Prostaglandins Other Lipid Mediat* **77**: 111–122.

Wallace MJ, Martin BR, DeLorenzo RJ (2002). Evidence for a physiological role of endocannabinoids in the modulation of seizure threshold and severity. *Eur J Pharmacol* **452**: 295–301.

White R, Hiley CR (1998). The actions of the cannabinoid receptor antagonist, SR 141716A, in the rat isolated mesenteric artery. *Br J Pharmacol* **125**: 689–696.

Yu M, Ives D, Ramesha CS (1997). Synthesis of prostaglandin E_2 ethanolamide from anandamide by cyclooxygenase-2. *J Biol Chem* **272**: 21181–21186.